Korean J. Chem. Eng., **31**(6), 1043-1048 (2014)
DOI: 10.1007/s11814-014-0025-3

pISSN: 0256-1115
eISSN: 1975-7220

Ionic liquids [EMIM][BF$_4$], [EMIM][Otf] and [BMIM][Otf] as corrosion inhibitors for CO$_2$ capture applications

Anissa Acidi*, Muhammad Hasib-ur-Rahman, Faiçal Larachi**, and Azzedine Abbaci*,***,†**

*Laboratoire de Synthèse et de Biocatalyse Organique, Département de Chimie,
Universit Badji Mokhtar, Sidi Amar, 23200, Annaba, Algeria
**Département de Génie Chimique, Université de Laval, Québec QC, G1 V 0A6, Canada
***National Research Center of Welding and Non Destructive Testing,
Route de Dély-Ibrahim - BP 64, Cheraga, Algiers 16000, Algeria

(*Received 7 October 2013 • accepted 20 January 2014*)

Abstract−We present the viability of using thermally stable, practically non-volatile ionic liquids as corrosion inhibitors in aqueous monoethanolamine systems. Carbon steel 1020, which is widely used as a construction material in CO$_2$ capture plants, has been taken as a test material. Corrosion inhibition capabilities of typical room-temperature ionic liquids constituting imidazolium cation in concentration range ≤3% in CO$_2$ capture applications were investigated. Electrochemical corrosion experiments using the potentiodynamic polarization technique for measuring corrosion current were carried out. Subsequent calculation of corrosion rate via Tafel fit was performed. The experimental findings suggest that the corrosion rate is significantly dependent on the process parameters, such as the CO$_2$ loading and the presence of oxygen. In addition, the value of the corrosion rate is sensitive to the type of ionic liquid added. Moreover, the results show that ionic liquids possess the ability of suppressing severe operational problems of corrosion in typical CO$_2$ capture plants to a reasonable extent (≥50%).

Keywords: Absorption, Carbon Dioxide, Carbon Steel, Monoethanolamine, Corrosion Rate, Tafel Fit, Ionic Liquids

INTRODUCTION

The unprecedented increases in the CO$_2$ emissions in the atmosphere have triggered the international community to take actions towards the protection of the environment. Incentive measures for using renewable and non-fossil energy sources that include energy from water, wind, sun, geothermal sources, and biomass sources such as energy crops are being taken. Although these sources of energies are benign to the environment and produce electricity, there can be negative environmental impacts on growth and safety of wildlife [1,2].

Post-combustion carbon dioxide capture and sequestration has attracted interest of several research groups as a measure for extenuation of global climate change. A very promising approach to reduce CO$_2$ emissions is its capture at a power plant, transport to an injection site, and its sequestration long-term storage in any of a variety of suitable geologic formations [3,4].

As a result, CO$_2$ capture has become an important part of the future power production. Current post-combustion CO$_2$ capture systems in power plants typically employ solvent based absorption followed by a desorption step, usually a stripping column, to strip off CO$_2$ and regenerate the solvent. The typical solvents used for this purpose are the amine based absorption agents, such as Monoethanolamine (MEA) [5-9].

The flue gas from power plants normally contains 12% in volume of CO$_2$ as well as nitrogen. CO$_2$ from flue gas is selectively absorbed in MEA solution through a chemical reaction in the absorption step. MEA has reasonable CO$_2$ capture capacity, low hydrocarbon solubility, reacts quickly with CO$_2$ and is relatively inexpensive, thus making it a popular choice in commercial processes. These advantages are associated with several disadvantages related to MEA that possesses high vapor pressure, which leads to fugitive emissions during regeneration and a corrosive nature of CO$_2$-captured product (carbamates/carbonates), which limits its use to dilute aqueous solutions. It also forms degradation products due to side reactions between some minor constituents of the flue gas.

Corrosion is considered one of the most severe operational problems in the CO$_2$ absorption processes using aqueous solutions of alkanolamines [10-14]. The volume of amine corrosion products depends on the corrosion rate; hence, it is important to keep the corrosion rate as low as possible. The corrosion rate increases with different factors, such as total amine concentration, CO$_2$ loading, solution temperature and the dissolved oxygen content [11,15]. Moreover, regardless of the amount of dissolved oxygen, the presence of heat-stable salts will also increase the corrosion rate [16].

Table 1 illustrates the different reactions involved in the process. Veawab et al. [17] and Brennecke and Maginn [18] have outlined the chemical reactions taking place into the bulk solution due to CO$_2$ absorption (reactions 1-5), due to corrosion (reactions 6-9), and due to formation of corrosion products (reactions 10 and 11).

This suggests that corrosion occurs due to anodic and cathodic reactions. The anodic reaction is iron dissolution (reaction 7) while the cathodic reactions are reduction of oxidizers present in the solution. In the absence of oxygen, possible primary corrosion (reactions 7-10) can occur.

Brennecke and Maginn [18] suggested that in the presence of

[†] To whom correspondence should be addressed.
E-mail: azzedine.abbaci@univ-annaba.dz

Table 1. Chemical reactions taking place into the bulk solution due to CO_2 absorption, corrosion and formation of corrosion products

Chemical reactions	Reaction type	
$2\ H_2O \leftrightarrow H_3O^+ + OH^-$	Solvolysis	(1)
$2\ H_2O + CO_2 \leftrightarrow H_3O^+ + HCO_3^-$	Carbonic acid 1st acidity	(2)
$H_2O + HCO_3^- \leftrightarrow H_3O^+ + CO_3^{-2}$	Carbonic acid 2nd acidity	(3)
$RNH_3^+ + H_2O \leftrightarrow RNH_2 + H_3O^+$	Amine conjugated acid deprotonation	(4)
$HOCH_2CH_2NH_2\ (aq) + CO_2(g) \leftrightarrow HOCH_2CH_2NHCOOH$	Carbamic acid formation	(5)
$RNHCOO^- + H_2O \leftrightarrow RNH_2 + HCO_3^-$	Carbamate hydrolysis	(6)
$Fe \leftrightarrow Fe^{+2} + 2e^-$	Iron (1/2-reaction) oxidative dissolution	(7)
$2\ H_3O^+ + 2e^- \leftrightarrow 2\ H_2O + H_2(g)$	Hydroxonium (1/2 reaction) reduction	(8)
$2\ HCO_3^- + 2e^- \leftrightarrow 2\ CO_3^{-2} + H_2(g)$	Reduction of bicarbonate ion	(9)
$2\ H_2O + 2e^- \leftrightarrow 2\ OH^- + H_2(g)$	Reduction of undissociated water	(10)
$Fe^{+2} + 2OH^- \leftrightarrow Fe(OH)_2$	Formation of ferrous hydroxide	(11)
$Fe^{+2} + CO_3^{-2} \leftrightarrow FeCO_3$	Formation of ferrous carbonate	(12)

oxygen there is an increase of the corrosion rate that can be explained by the increase in the oxidizer concentration in the solution. The O_2 dissolved into solution receives electrons as shown in the following reaction.

$$\text{Reduction of dissolved } O_2\text{: } O_2 + 2H_2O + 4e^- \leftrightarrow 4\ OH^- \qquad (13)$$

A number of corrosion inhibitors such as arsenic and vanadium have been used for corrosion prevention and control. However, due to their toxicity to humans and to the environment, it is therefore necessary to look for potential low-toxic corrosion inhibitors for the CO_2 absorption process [19]. Ionic liquids (ILs) are a class of organic salts that are characterized by their liquidity over a wide range of temperatures. They are also known to have unique properties such as negligible vapor pressures, tunable physical and chemical properties, and high thermal stabilities [20,21]. These properties make ILS a potential replacement for many conventional volatile organic solvents in reaction and separation processes [22]. Therefore, ionic liquids (ILs) can be used as a substitute for conventional corrosion inhibitors.

Previous studies addressing the assessment of corrosion inhibition in O_2-MEA-H_2O systems have been performed by Soosaiprakasam and Veawab [23]. More recently, Hasib-ur-Rahman et al. [24] tested and investigated alkanolamine/room-temperature ionic liquid (RTIL) systems by systematically probing the effect of amine/RTIL type, process temperature, CO_2 loading, presence/absence of oxygen in flue gas, as well as the influence of water content. Furthermore, the corrosion mechanism at the interface between the carbon steel surface and the CO_2 loaded MEA aqueous solution was described in previous work published in the literature [16, 25].

We investigated three promising ionic liquids with small alkyl chains, namely, 1-ethyl-3-methylimidazolium tetrafluoro borate [EMIM][BF_4], 1-ethyl-3-methylimidazolium trifluoromethanesulfonate [EMIM][Otf] and 1-Butyl-3-Methylimidazolium Trifluoromethanesulfonate [BMIM][Otf], to determine their corrosion inhibition ability. The electrochemical linear polarization technique and Tafel fit were used to determine the corrosion rates. This study was conducted in the group "Procédés et Matériaux pour des Energies Durables of Universit Laval (Canada) and Laboratoire de Synthèse et de Biocatalyse Organique, of Universit Badji Mokhtar (Algeria) in 2010-2012.

MATERIALS AND METHODS

1. Materials

A cylindrical specimen made from carbon steel 1020 for conducting corrosion tests having a chemical composition of 0.20% carbon, 0.50% manganese, 0.04% phosphorus, 0.05% sulfur, was used as working electrode in this study. For all the experiments, the specimen was polished by a wet grinding with 600 grit abrasive silicon carbide papers and deionized water, then degreased with high purity acetone, rinsed with deionized water and then dried in hot air. An aqueous solution of MEA with a 10% weight concentration was prepared from a 99% MEA reagent and deionized water. The solution was loaded with the desired CO_2 loading by passing the gas through the solution. The prepared MEA solution was subsequently analyzed before and after adding ionic liquids as corrosion inhibitors. Table 2 shows the ionic liquids used and the tested parameters and conditions for inhibited MEA-H_2O-CO_2-RTILs systems in this work.

2. Electrochemical Setup

The electrochemical experiment was performed using a corrosion cell with a three electrode assembly comprising a cylindrical working electrode made of carbon steel 1020 with a surface area

Table 2. Tested parameters and conditions for inhibited MEA-H_2O-CO_2-RTILs systems

IL	Stoichiometry	Concentration (wt%)
[EMIM][BF_4]	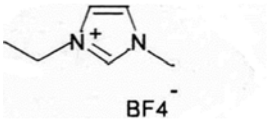	3.0
[BMIM][Otf]	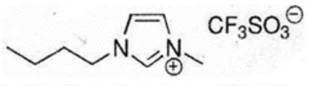	3.0
[EMIM][Otf]	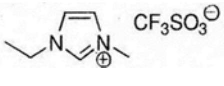	3.0
MEA		10
Loading (mol CO_2/mol MEA)		0.40

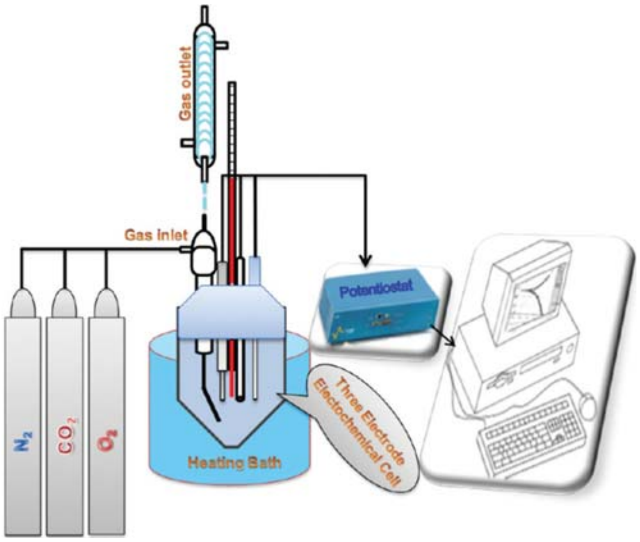

Fig. 1. Schematic diagram of electrochemical corrosion setup taken from Hasib-ur-Rahman et al. [24].

of 0.786 cm^2, an Ag/AgCl as a reference electrode and platinum (Pt) counter electrode as shown in Fig. 1. Carbon steel 1020 and Fe balanced was used as the specimen working electrode to study the corrosive behavior of aqueous alkanolamines in presence/absence of RTIL inhibitors. The electrochemical experiment began with a cathodic cleaning at −1.1 V for 5 min to remove any residual air formed oxides on the working electrode by creating a virtually clean surface [24].

The gas supply set consisted of a CO$_2$ gas cylinder. The gas was introduced into the corrosion cell 30 min before starting the polarization in order to saturate the MEA aqueous solution. The corrosion cell was connected to a potentiostatic system, which was in turn connected to a computer with data acquisition software to record and analyze the produced corrosion data as shown in Fig, 1. The polarization scan was initiated after a steady state open-circuit potential was attained. Potentiodynamic polarization and Tafel plot were used for corrosion measurement. The polarization curve of carbon steel in CO$_2$ loaded MEA aqueous solution is shown in Fig. 2.

For electrochemical corrosion tests, CO$_2$ loading was determined by a Chittick apparatus using the titration method. To release the captured gas, small samples were withdrawn from the electrochemical cell and titrated against a standard solution of HCl (1 M) by means of methyl orange indicator. The actual quantity of CO$_2$ loading was calculated subsequently from the volume of CO$_2$ evolved. In the case of aqueous samples, the CO$_2$ partial pressure was corrected for the vapor pressure of water.

Linear polarization resistance (LPR) curves were recorded at a constant polarization value of scan rate of 0.16 mVs^{-1} starting from a cathodic potential of −250 mV to an anodic potential of +250 mV (versus open circuit potential). During electrochemical experimentation, 500 rpm of rotation speed was maintained for the working electrode. The values of corrosion rates represent an average value from repetition tests values with an uncertainty of 5%.

A Tafel plot involved the polarization scan from cathodic to anodic direction in the potential range of ±250 mV. The Tafel extrapolation technique [14,17,23] was used to estimate corrosion current density (I$_{corr}$) which was converted to corrosion rate (CR) using the following expression [24,26]:

$$\mathrm{CR} = \frac{\mathrm{k} \cdot \mathrm{I}_{corr} \cdot \mathrm{E}_W}{\rho \cdot \mathrm{A}} \tag{14}$$

where CR is the corrosion rate in milli-inch per year (mpy), E$_W$ is the equivalent weight of the specimen in g/equivalent, A is the area (in contact with experimental fluid) of working electrode in cm^2 and ρ is the density of the specimen in g/cm^3 and k=1.288.10^5.

RESULTS AND DISCUSSION

1. Corrosion Behaviour in the Absence of Inhibitors

Polarization behavior of carbon steel immersed in an aqueous solution of MEA retaining CO$_2$ loading of 0.4 mole CO$_2$ per mole MEA at 25 °C showed that during most of the potential range applied, the carbon steel specimen was clearly in the active state. The corrosion mechanism at the interface between the carbon steel surface and the CO$_2$-loaded MEA aqueous solution was examined to interpret the typical behavior [27,28] as shown in Fig. 2.

High corrosion due to anodic reaction especially iron dissolution produces ferrous ion Fe^{+2} (reaction 7) and reduction of oxidizing agent (mainly bicarbonate (HCO_3^-). These two electrochemical reactions lead to the formation of ferrous carbonate ($FeCO_3$) as corrosion products.

Furthermore, O$_2$ has an influence on the corrosion behavior of

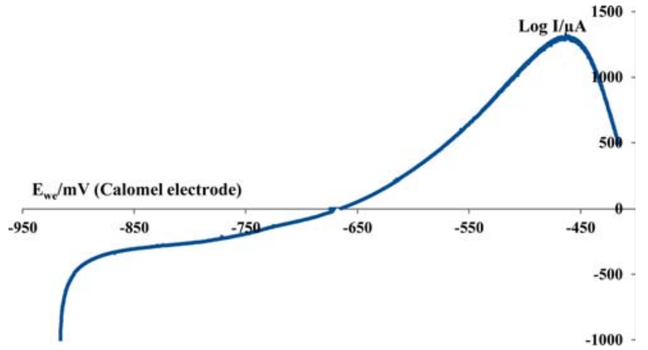

Fig. 2. Polarization behaviour of carbon steel in CO$_2$ loaded MEA aqueous solution.

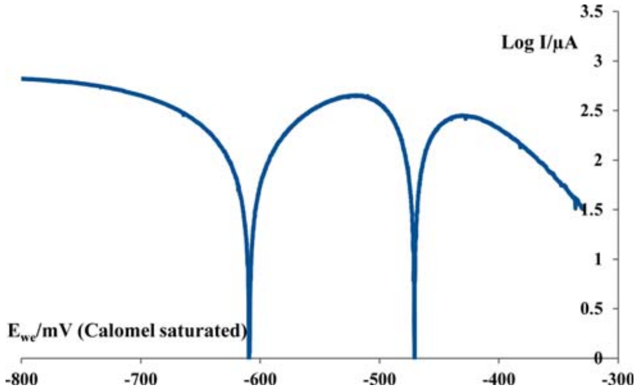

Fig. 3. Typical behaviour of carbon steel in CO$_2$+O$_2$ loaded MEA aqueous solution.

Table 3. Corrosion rates values of carbon steel immersed in CO_2-loaded MEA aqueous solution with 3% by weight of different ILs/ as well as for systems with and without corrosion inhibitors

Medium	CR (mpy)
[EMIM][BF_4]	0.30
[EMIM][Otf]	92.5
[BMIM][Otf]	104.9
CO_2/MEA aq.	82.6
CO_2+O_2/MEA aq.	113.2
CO_2+O_2/MEA+[EMIM][BF_4]	0.22
CO_2+O_2/MEA [EMIM][Otf]	2.65

carbon steel. The cyclic polarization curve of carbon steel in an aqueous solution of 10% MEA containing CO_2 at room temperature in the presence of O_2 is shown in Fig. 3. The increase in corrosion rate is due to an increase in the oxidizer concentration resulting from the dissolution of O_2 into the solution and subsequently undergoing reduction by addition of electrons (reaction 12), which in turn induces a greater rate of iron dissolution and acceleration of corrosion process.

2. Corrosion Behavior in the Presence of Inhibitors

The results of the corrosion rates for the three ionic liquids are presented in Table 3; it shows the corrosion rates of the carbon steel immersed in the CO_2-loaded MEA aqueous solution with the three different ionic liquids as corrosion inhibitors at 3% by weight. From these results it is clear that the best corrosion inhibition capability can be attributed to the ionic liquid [EMIM][BF_4]. In addition, Table 3 shows the corrosion rates values for the different systems used in this work with and without corrosion inhibitors in the presence of either H_2O or O_2 or both simultaneously. Copper carbonate $CuCO_3$ has the ability to reduce the corrosion rate of carbon steel below 0.25 mpy with an inhibition efficiency of at 80% [29]; this result is to be compared with the value of the corrosion rate found in this work 0,22 mpy for CO_2+O_2/MEA+[EMIM][BF_4] system. The inhibition performance of $CuCO_3$ is, however, reduced with degradation [14]. Sodium metavanadate $NaVO_3$ has been rejected as an inhibitor because it is a toxic/hazardous substance [29].

Figs. 4 and 5 present the effect of the [EMIM][BF_4] as a corrosion inhibitor on the polarization behavior of carbon steel in CO_2 loaded MEA aqueous solution; it is shown that the inhibitor has a considerable effect on the corrosion rate. The presence of [EMIM][BF_4] in CO_2/Amine aqueous solution decreases the current density to I_{corr}=0.429 μA showing good inhibition efficiency. This also suggests that the protective film of the inhibitor formed on the carbon steel surface tends to be stable. It is clear from Table 3 that MEA+[EMIM][BF4] still shows the best corrosion inhibition in the presence of CO_2/H_2O. This inhibition feature decreases in the presence of O_2.

Higher corrosion potential in the presence of inhibitor implies an inhibition effect of [EMIM][BF_4] on the $MEACOO^-$ induced corrosion. This effect can be attributed to the adsorption of anionic inhibitor on carbon steel surface by complex interactions with positively charged electrode surface, which hinders the access of $MEACOO^-$ to the steel surface and subsequently impedes local corrosion.

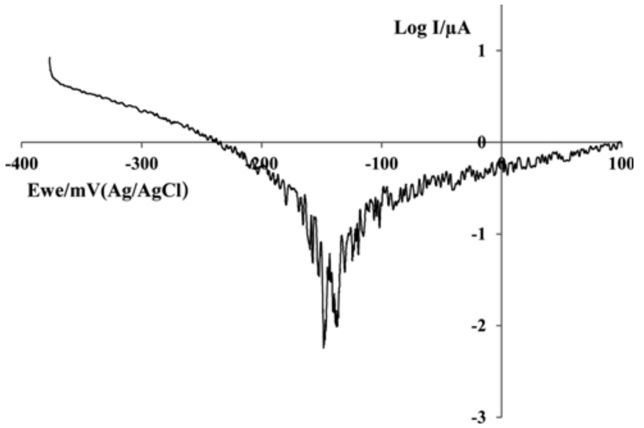

Fig. 5. Effect of the [EMIM][BF_4] as corrosion inhibitor on polarization behaviour of carbon steel in CO_2 loaded MEA aqueous solution.

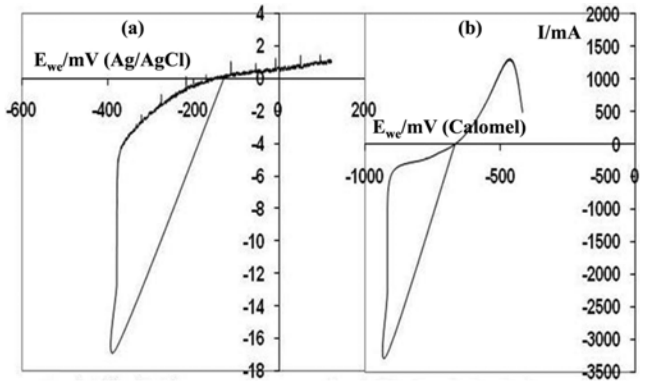

Fig. 4. Polarization behavior of carbon steel in CO_2 loaded MEA aqueous solution (a): with [EMIM][BF_4] (b) without [EMIM][BF_4].

3. Typical Corrosion Inhibition in the Presence of O_2

Hasib-ur-Rahman and coworkers [24] studied the corrosion phenomena in amine/room-temperature ionic liquid blends. Such systems comprised alkanolamine/s (MEA, 2-amino-2-methyl-1-propanol, diethanolamine, N-methyldiethanolamine) and hydrophilic room-temperature ionic liquid ([BMIM][BF_4], [EMIM][BF_4], and [EMIM]

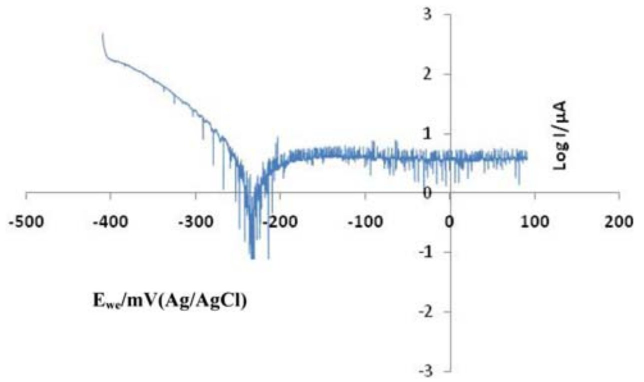

Fig. 6. Effect of the [EMIM][BF_4] as corrosion inhibitor on polarization behavior of carbon steel in CO_2+O_2 loaded MEA aqueous solution.

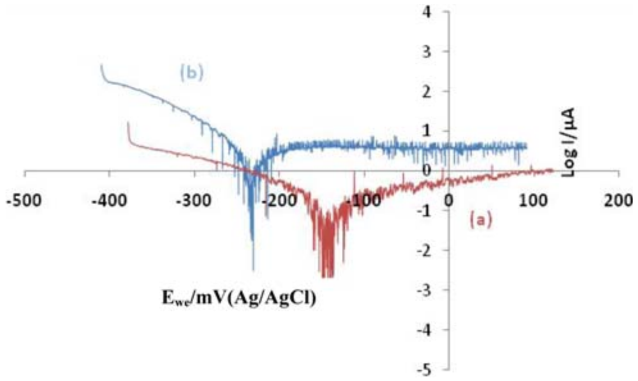

Fig. 7. Polarization behavior of carbon steel in (a): CO$_2$ loaded MEA aqueous solution and (b) CO$_2$+O$_2$ loaded MEA aqueous solution with [EMIM][BF$_4$] as corrosion inhibitor.

[Otf]). They systematically probed the effect of amine/RTIL type, process temperature, CO$_2$ loading, presence/absence of oxygen in flue gas, as well as the influence of water content. They concluded that [EMIM][BF$_4$] and [BMIM][BF$_4$] ionic liquids not only exhibited excellent corrosion control in the pure state but also demonstrated a similar trend in combination with alkanolamines. However, pure [EMIM][Otf] was very corrosive toward the electrode surface, primarily due to the presence of acidic impurities.

The effect of [EMIM][BF$_4$] as corrosion inhibitor on polarization behavior of carbon steel in CO$_2$ loaded MEA aqueous solution and CO$_2$+O$_2$ loaded MEA aqueous solution is shown in Figs. 6 and 7, respectively. Both polarization behaviors of carbon steel in the CO$_2$ loaded MEA aqueous solution in, and in the CO$_2$+O$_2$ loaded MEA aqueous solution with [EMIM][BF$_4$] as corrosion inhibitor, are illustrated in Fig. 7(a) and in Fig. 7(b); the corrosion rate is significantly sensitive to the presence of O$_2$, and the value of the corrosion current density is found to be I_{corr}=0.976 μA, thus increasing the corrosion rate to a value of CR=2.6451 mpy. Note that the presence of [EMIM][BF$_4$] caused a positive shift of the corrosion potential; therefore, [EMIM][BF$_4$] might be considered as an anodic inhibitor as illustrated in Fig. 7.

4. Effect of of the pH on Corrosion Rate

To examine the effect of the pH solution change in the presence/absence of the ionic liquid inhibitor, Table 4 presents the different pH values found. It is evident that in the absence of any inhibitor the pH value decreases from 11.25 to 8.11 because CO$_2$ is an acid gas, while in the presence of the [EMIM][BF$_4$] inhibitor the pH does not vary considerably.

5. Effect of of the Viscosity on Corrosion Rate

In the present work, the ionic liquids [EMIM][BF$_4$], [EMIM][Otf] and [BMIM][Otf] were not tested as corrosion inhibitors alone, but in the presence of an aqueous medium, namely, the aqueous monoethanolamine systems. The expected results are quite different from those of Hasib-ur-Rahman and Larachi [30]; here we found that the ILs with lowest viscosity value (Table 5) is the most effective in preventing corrosion in the presence of aqueous media, for the simple reason that the IL with lowest viscosity, namely [EMIM][BF$_4$], is the most adsorbed one by the metal and thence forms a surface protective films of [EMIM][BF$_4$]. This behavior enables the RTIL to safeguard the metal surface effectively. This fact can be verified from comparing the results presented in Table 3 with the data quoted in Table 5. The more viscous the IL is, the less its corrosion rate becomes.

Table 5. Viscosity values of the ionic liquids used (m Pa·s)^a

[EMIM][BF$_4$]	34.0
[EMIM][Otf]	39.8
[BMIM][Otf]	109.0

^{a}at 25 °C

CONCLUSION

This work reports the use of ionic liquids as additives in aqueous solutions of alkanolamines to examine their corrosion inhibiting effect. The corrosion rate of carbon steel 1020 in alkanolamine-RTIL solutions was studied. Inhibition efficiency decreases in the order [EMIM][BF$_4$], [EMIM][Otf], and [BMIM][Otf]. Furthermore, under similar CO$_2$ loading condition, the corrosion rate varies with the IL type added and the oxygen load has considerable impact on the system corrosiveness. [EMIM][Otf] and [BMIM][Otf] showed poor inhibition ability compared to [EMIM][BF$_4$], which may be due the stronger interaction of carbon dioxide to [EMIM][BF$_4$]. Room temperature ionic liquids (RTILs) could be promising solvents as corrosion inhibitors in CO$_2$ capture application. These results show the possibility of using [EMIM][BF$_4$] as an excellent corrosion inhibitor. This aspect needs more extensive investigations using other types of ionic liquids in order to understand thoroughly the real mechanism of inhibition either by the anion or cation with different concentrations. Presently, the main constraint in using ionic liquids for CO$_2$ capture is its very high cost. As a result, its use is limited only to laboratory scales.

ACKNOWLEDGEMENTS

The authors gratefully acknowledge financial support from the Laboratoire de Synthèseet de Biocatalyse Organique/PNR DGRST Algeria: PNR contract no. 1/2011, avenant no. 88/2011, and FL Canada Research Chair "Green Processes for Cleaner and sustainable Energy," Universit Laval, Québec, Canada.

NOMENCLATURE

CR : the corrosion rate, milli-inch per year [mpy]
i_{corr} : the corrosion current, Ampere
E_w : the equivalent weight of metal specimen, gram per equivalent

Table 4. pH values in the presence/absence of inhibitor

System	MEA-H$_2$O	MEA-H$_2$O+CO$_2$	MEA-H$_2$O+CO$_2$+[EMIM][BF$_4$]	MEA-H$_2$O+CO$_2$+O$_2$+[EMIM][BF$_4$]
pH	11,25	8,11	7,70	7,53

ρ : the density of metal [g cm^{-3}]

A : the area (in contact with experimental fluid) of the rotating disk working electrode [cm^2]

Abbreviation

IL : ionic liquid

RTIL : room temperature ionic liquid

[EMIM][BF$_4$] : 1-ethyl-3 methylimidazolium tetrafluoro borate

[EMIM][Otf] : 1-ethyl-3methylimidazolium trifluoromethanesulfonate

[BMIM][Otf] : 1-butyl-3-Methylimidazolium Trifluoromethanesulfonate

MEA : monoethanolamine

REFERENCES

1. M. C. Heller, G. A. Keoleian and T. A. Volk, *Biomass Bioenergy*, **25**, 147 (2003).
2. K. G. Knudsen, B. H. Cooper and H. Topsoe, *Appl. Catal. A: Gen*., **189**(2), 205 (1999).
3. J. D. Figueroa, T. Fout, S. Plasynski, H. McIlvried and R. D. Srivastava, *Int. J. Greenhouse Gas Control*, **2**, 9 (2008).
4. S. M. Benson and D. R. Cole, *Element*., **4**, 325 (2008).
5. H. Chang and C. M. Shih, *Sep. Sci. Technol*., **40**, 877 (2005).
6. M. S. Jassim and G. T. Rochelle, *Ind. Eng. Chem. Res*., **45**(8), 2465 (2006).
7. A. Bello and R. O. Idem, *Ind. Eng. Chem. Res*., **45**(8), 2569 (2006).
8. G. S. Goff and G. T. Rochelle, *Ind. Eng. Chem. Res*., **43**(20), 6400 (2004).
9. L. Kucka, I. Müller, E. Y. Kenig and A. Górak, *Chem. Eng. Sci*., **58**(16), 3571 (2003).
10. I. Ahamad, C. Gupta, R. Prasad and M. A. Quraishi, *J. Appl. Electrochem*., **40**(12), 2171 (2010).
11. B. Hamah-Ali, B. Si Al, R. Yusoff and M. Kheirodin Aroua, *Int. J. Electrochem. Sci*., **6**, 181 (2011).
12. K. F. Khaled, A. El-mghraby, O. B. Ibrahim, O. A. Elhabib and A. M. I. Magdy, *J. Mater. Environ. Sci*., **1**(3), 139 (2010).
13. J. Gao, S. Wang, C. Sun, B. Zhao and C. Chen, *Ind. Eng. Chem. Res*., **51**(19), 6714 (2012).
14. I. R. Soosaiprakasam and A. Veawab, *Energy Procedia*., **1**, 225 (2009).
15. N. Kladkaew, R. Idem, P. Tontiwachwuthikul and C. Saiwan, *Ind. Eng. Chem. Res*., **48**(23), 10169 (2009).
16. M. Hasib-ur-Rahman, M. Siaj and F. Larachi, *Chem. Eng. Process*., **49**, 313 (2010).
17. A. Veawab, P. Tontiwachwuthikul and A. Chakma, *Ind. Eng. Chem. Res*., **38**, 3917 (1999).
18. J. F. Brennecke and E. J. Maginn, *AIChE J*., **47**, 2384 (2001).
19. T. P. T. Pham, C. W. Cho and Y. S. Yun, *Water Res*., **44**, 352 (2010).
20. T. Tsuda and C. L. Hussey, *Interface*, **16**, 42 (2007).
21. S. Zhang, N. Sun, X. He, X. Lu and X. Zhang, *J. Phys. Chem. Ref. Data*, **35**(4), 1475 (2006).
22. A. Veawab, P. Tontiwachwuthikul and A. Chakma, *Ind. Eng. Chem. Res*., **40**(2), 4771 (2001).
23. I. R. Soosaiprakasam and A. Veawab, *Int. J. Greenhouse Gas Control*, **2**, 553 (2008).
24. M. Hasib-ur-Rahman, H. Bouteldja, P. Fongarland, M. Siaj and L. Larachi, *Ind. Eng. Chem. Res*., **51**(26), 8711 (2012).
25. S. Martin, H. Lepaumier, D. Picq, J. Kittel, T. de Bruin and A. Faraj, P. L. Carrette, *Ind. Eng. Chem. Res*., **51**(8), 6283 (2012).
26. M. A. M. Ibrahim, M. Messali, Z. Moussa, A. Y. Alzahrani, S. N. Alamry and B. Hammouti, *Port. Electrochim. Acta*, **29**, 375 (2011).
27. M. Uerdingen, C. Treber, M. Balser, Schmitt and C. Werner, *Green Chem*., **7**, 321 (2005).
28. I. Perissi, U. Bardi, S. Caporali and A. Lavacchi, *Corros. Sci*., **48**, 2349 (2006).
29. J. Kittela, R. Idemb, D. Gelowitzb, P. Tontiwachthikulb, G. Parraina and A. Bounneaua, *Energie Procedia*, **1**, 791 (2009).
30. M. Hasib-ur-Rahman and F. Larachi, *Ind. Eng. Chem. Res*., **52**(49), 17682 (2013).